



ARL-TN-0671 • MAY 2015



Inspection Correlation Study of Ultrasonic- Based In Situ Structural Health Monitoring Monthly Report for December 2014–January 2015

by Eliseo E Iglesias, Robert A Haynes, and Chi-yu Shiao

Approved for public release; distribution is unlimited.

NOTICES

Disclaimers

The findings in this report are not to be construed as an official Department of the Army position unless so designated by other authorized documents.

Citation of manufacturer's or trade names does not constitute an official endorsement or approval of the use thereof.

Destroy this report when it is no longer needed. Do not return it to the originator.



Inspection Correlation Study of Ultrasonic-Based In Situ Structural Health Monitoring Monthly Report for December 2014–January 2015

by Eliseo E Iglesias
University of Texas San Antonio

and

Robert A Haynes and Chi-yu Shiao
Vehicle Technology Directorate, ARL

REPORT DOCUMENTATION PAGE				Form Approved OMB No. 0704-0188	
<p>Public reporting burden for this collection of information is estimated to average 1 hour per response, including the time for reviewing instructions, searching existing data sources, gathering and maintaining the data needed, and completing and reviewing the collection information. Send comments regarding this burden estimate or any other aspect of this collection of information, including suggestions for reducing the burden, to Department of Defense, Washington Headquarters Services, Directorate for Information Operations and Reports (0704-0188), 1215 Jefferson Davis Highway, Suite 1204, Arlington, VA 22202-4302. Respondents should be aware that notwithstanding any other provision of law, no person shall be subject to any penalty for failing to comply with a collection of information if it does not display a currently valid OMB control number.</p> <p>PLEASE DO NOT RETURN YOUR FORM TO THE ABOVE ADDRESS.</p>					
1. REPORT DATE (DD-MM-YYYY) May 2015		2. REPORT TYPE Final		3. DATES COVERED (From - To) 1 December 2014–31 January 2015	
4. TITLE AND SUBTITLE Inspection Correlation Study of Ultrasonic-Based In Situ Structural Health Monitoring Monthly Report for December 2014–January 2015				5a. CONTRACT NUMBER	
				5b. GRANT NUMBER	
				5c. PROGRAM ELEMENT NUMBER	
6. AUTHOR(S) by Eliseo E Iglesias, Robert A Haynes, and Chi-yu Shiao				5d. PROJECT NUMBER	
				5e. TASK NUMBER	
				5f. WORK UNIT NUMBER	
7. PERFORMING ORGANIZATION NAME(S) AND ADDRESS(ES) US Army Research Laboratory ATTN: RDRL-VTM Aberdeen Proving Ground, MD 21005-5066				8. PERFORMING ORGANIZATION REPORT NUMBER ARL-TN-0671	
9. SPONSORING/MONITORING AGENCY NAME(S) AND ADDRESS(ES)				10. SPONSOR/MONITOR'S ACRONYM(S)	
				11. SPONSOR/MONITOR'S REPORT NUMBER(S)	
12. DISTRIBUTION/AVAILABILITY STATEMENT Approved for public release; distribution is unlimited.					
13. SUPPLEMENTARY NOTES					
14. ABSTRACT This report provides the current status on activities pertaining to the research project Inspection Correlation Study of Ultrasonic-Based In Situ Structural Health Monitoring. The project members, Dr Robert Haynes, research engineer at the US Army Research Laboratory's Vehicle Technology Directorate (ARL/VTD), and postgraduate intern Eli Iglesias, working alongside Dr Michael Shiao, research engineer at ARL/VTD, are conducting this inspection correlation study via ultrasonic-based inspection of fatigue crack growth in aluminum 7075-T6 dogbone specimens. Acellent Technologies, Inc., is supporting this project through providing hardware, software, and training for the in situ ultrasonic inspection and damage signal analysis. Reporting period is 1–17 December 2014 and 12–31 January 2015.					
15. SUBJECT TERMS structural health monitoring, probabilistics, fatigue damage, guided waves, Lamb waves					
16. SECURITY CLASSIFICATION OF:			17. LIMITATION OF ABSTRACT UU	18. NUMBER OF PAGES 30	19a. NAME OF RESPONSIBLE PERSON Robert A Haynes
a. REPORT Unclassified	b. ABSTRACT Unclassified	c. THIS PAGE Unclassified			19b. TELEPHONE NUMBER (Include area code) 410-278-8035

Contents

Contents	iii
List of Figures	iv
1. Introduction	1
2. Objectives	1
3. Approach and Experimental Procedure: Stable Fatigue Crack Growth	2
3.1 Dogbone Specimen	2
3.2 Fatiguing Parameters	3
3.3 Summary of Experiment Procedure	3
3.4 SHM Ultrasonic Scan	4
4. Crack-Length Measurement	7
5. Results: DB1	10
5.1 Crack-Length Images	10
5.2 Damage Index Algorithms	10
5.3 Future Work	13
6 February 2015 Proceedings	13
7. References	14
Appendix A. Experimental Procedure	15
Appendix B. Setup for Crack Image Capture for Dogbone 2	19
List of Symbols, Abbreviations, and Acronyms	23
Distribution List	24

List of Figures

Fig. 1 Specimen layout	3
Fig. 2 Procedure	4
Fig. 3 Hardware setup	4
Fig. 4 Actuator-sensor paths	5
Fig. 5 Example pitch signal	6
Fig. 6 Example catch signal	6
Fig. 7 Scatter signal.....	7
Fig. 8 Camera setup	8
Fig. 9 Crack propagation area	8
Fig. 10 Visual calibration piece	9
Fig. 11 Example visual measurement	9
Fig. 12 DB1 measured crack length.....	10
Fig. 13 Scatter wave DI	11
Fig. 14 Pearson's coefficients DI.....	12
Fig. B.1 Camera translation stage	20
Fig. B.2 Bottom view of camera translation stage.....	20
Fig. B.3 White-out application.....	21

1. Introduction

In current industry and defense agencies there is a push for more-efficient (cost and time) inspection, maintenance, and flight cycle of air vehicles. Current inspections and maintenance of air vehicles have become increasingly expensive both economically and in time consumption, resulting in lower vehicle readiness and availability. Condition-based maintenance (CBM) could provide a way to reduce cost and be an effective tool for making decisions about the inspection, maintenance, and flight of air vehicles. CBM is composed of 3 basic methodologies: prognostics and diagnostics for components, usage monitoring, and fatigue life management.¹ Over the last 20 years, nondestructive inspection (NDI) methods have been developed to assist in the diagnosis and prognosis of air vehicles. In addition, probabilistic structural risk assessment (PSRA) tools have been developed (e.g., RPI, DARWIN) to calculate the probability of detection (POD) and risk of these NDI methods.

Structural health monitoring (SHM) uses similar NDI methods; however, the goal is to apply in situ NDI sensors to allow for semiautonomous inspection and faster inspection time. Such developments could reduce time on the ground, inspection time, and cost. However, the PSRA of SHM has not been fully developed. NDI PSRA inspections are considered independent events (sensors are not in situ) while in SHM inspection events are susceptible to dependent relationships between inspection events. This project attempts to develop a better understanding of the correlations not only between inspection events, but between crack propagation and applied piezoelectric induced vibrations.

2. Objectives

- Perform SHM experiments to general signals with and without damages and measure corresponding damage size.
- Identify signal features that can be used to correlate damage size.
- Perform linear regression with correlated measuring data, and quantify inspection correlation

The first objective requires development of a controlled crack growth procedure. In this procedure, stable incremental crack growth is achieved, and at every interval of cycle fatigue an induced ultrasonic elastic vibration (via piezoelectric transducers [PZTs]) propagates through the dogbone specimen. A receiver PZT picks up the vibration signal that carries damage information as the crack length

increases. After acquiring damage signal and crack growth data (via visual inspections), the next task applies a linear regression algorithm between the 2 that produces residual data. In the second objective the residual data guides the analysis toward incorporating correlated variables in the linear regression algorithm. Lastly, if significant correlation is found in the residual data, changes can be made to the crack POD assessment of SHM, which will be explored after subsequent testing of aluminum (Al) 7075-T6 dogbone specimens.

This report for December 2014–January 2015 reviews the current experimental procedure for fatigue crack growth of Al 7075-T6 dogbone specimens and explores the results for dogbone 1 (DB1), the first dogbone specimen fatigued with SMART layers, provided by Acellent Technologies, Inc.

3. Approach and Experimental Procedure: Stable Fatigue Crack Growth

3.1 Dogbone Specimen

The specimens used for crack growth are Al 7075-T6 dogbones, which have a nominal thickness of 0.063 inch, ultimate tensile strength of 75 ksi, yield stress of 69.9 ksi, and modulus of elasticity of 10,400 ksi.² Figure 1 shows the dimensions of the dogbone, which was machined with a hole in the center to promote crack initiation and growth, and a crack propagation area and notch. To induce crack growth in approximately 30,000 cycles of fatigue loading, a notch cut was applied to the right of the hole in a direction perpendicular to the length of the specimen. The notch cut was administered by a jewelers saw blade 7 mil thick. The crack propagation area, shown in Fig. 1, is where the crack is expected to propagate due to the notch cut.

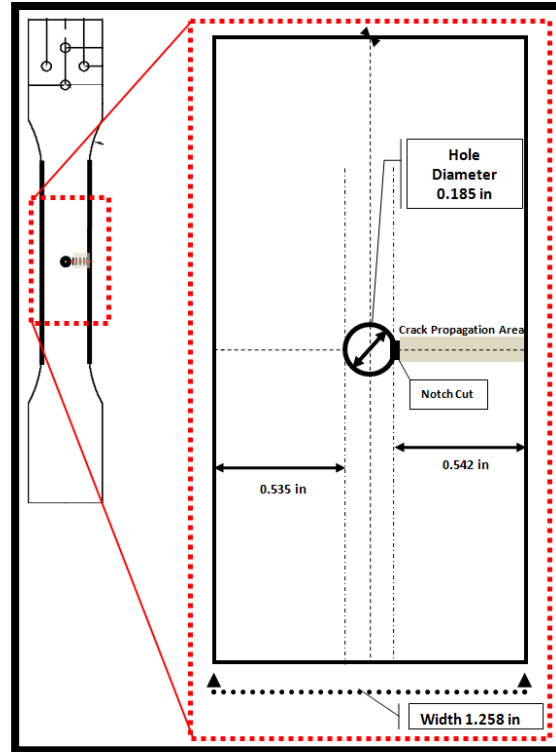


Fig. 1 Specimen layout

3.2 Fatiguing Parameters

According to Derriso³ the applied load should be determined by the strain limit of the adhesive used for the transducers. If the strain is high enough, debonding could occur. In DeSimio's US Air Force Research Laboratory study, the maximum stress level was calculated using limiting strain level of 1,500 microstrains.³ Using the geometrical dimensions of the dogbone this maximum stress is 107 MPa (15.6 ksi). For the preliminary experiments conducted before the time of this report, the cycle fatigue load of 1.23 kips (high) and 0.123 kips (low) ($R = 0.1$) was applied. In the DB1 experiment the high load was 5 kN and the low was 500 N. This was done to prevent debonding within the adhesive on the SMART layer patches attached by Acellent.

3.3 Summary of Experiment Procedure

A full version of the experimental procedure can be found in Appendix A, which details the proceedings for stable fatigue crack growth and the collection of damage signal and crack length measurement data. Figure 2 provides a summary of the procedure.

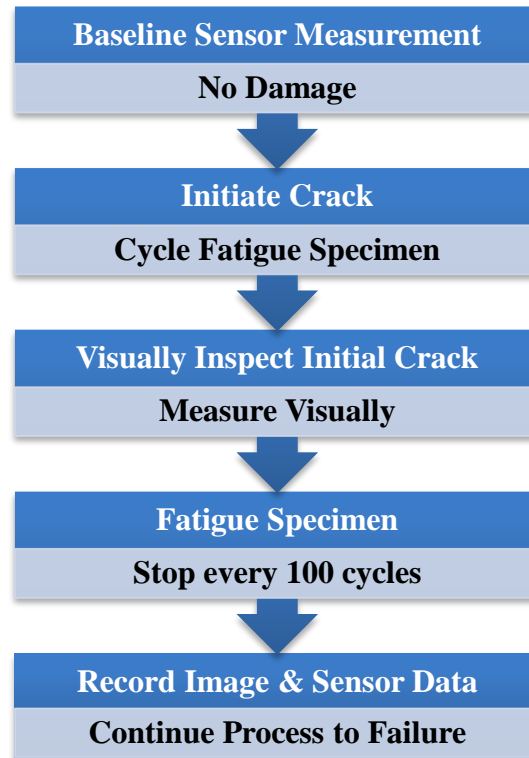


Fig. 2 Procedure

3.4 SHM Ultrasonic Scan

Acellent Technologies, Inc., provided the SMART layer patches that contain the PZT actuators designed to induce and detect ultrasonic elastic waves. They also provided the corresponding hardware, ScanGenie-II, needed to send and record the appropriate voltages for these ultrasonic waves. Figure 3 shows the general setup of the hardware and the SMART layer patches provided.

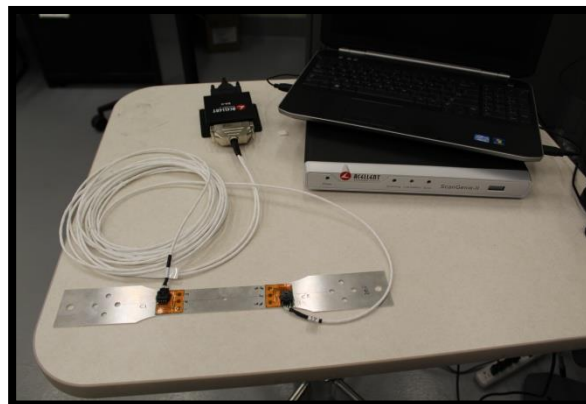


Fig. 3 Hardware setup

In the scanning procedure, the Acellent-provided software, SHM Patch, enables triggering and collection of ultrasonic elastic wave data. SHM Patch allows the user to specify the following parameters for the applied waves: type of wave induced, frequency of the wave, actuator-sensor paths, and averaging value (average damage signal of N signals applied). Figure 4 shows the different actuator-sensor paths for the current configuration.

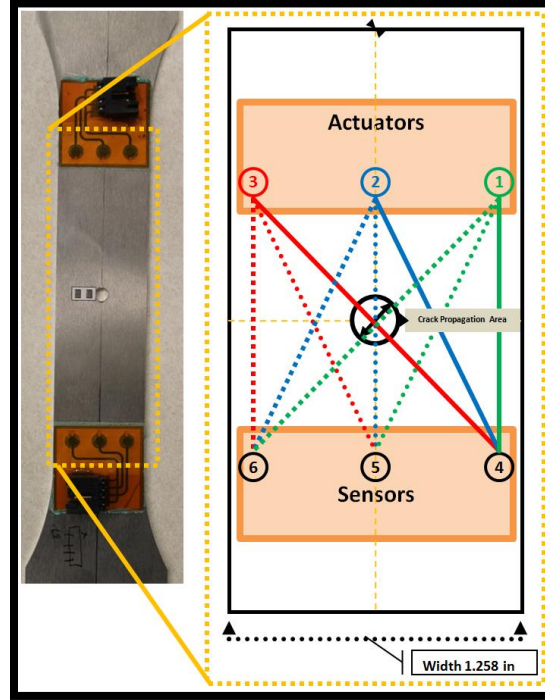


Fig. 4 Actuator-sensor paths

These paths do not represent propagation paths of the elastic waves but rather the order in which the Scan Genie-II hardware applies an ultrasonic wave and listens for the response. For example, path 2-4 applies a 250-kHz hamming window wave pulse to actuator 2 (blue) and receives a corresponding signal response exclusively from sensor 4. There are a total of 9 paths Scan Genie-II cycles through in every triggering of the scanning procedure.

The input signal into the actuators (1–3) is a 250-kHz hamming windowed wave pulse, 5 periods in length.

Figure 5 displays an example pitch signal (normalized and filtered by SHM Patch) actuators 1–3 induced into the Al dogbone. Sensors 4–6 detect and record the incoming elastic wave and its reflections (due to wave propagation). Figure 6 is an example “catch” signal.

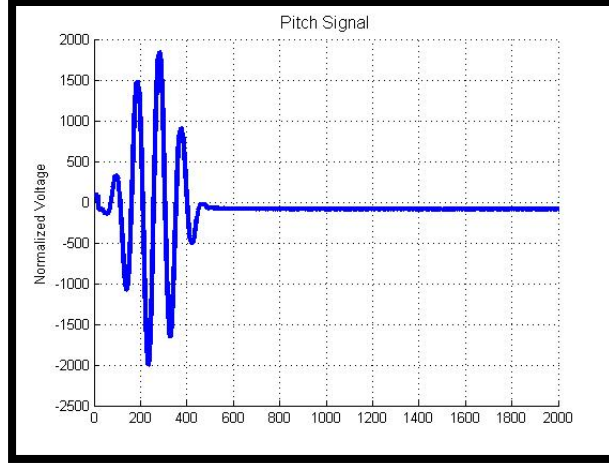


Fig. 5 Example pitch signal

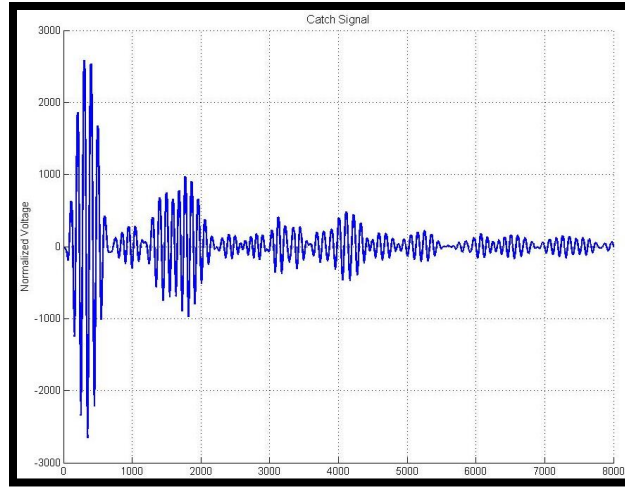


Fig. 6 Example catch signal

The catch signal contains not only the initial wave packet sent by the pitch signal, but also multiple reflections that could be the result of damage or natural boundaries in the dogbone. One way to determine damage behavior in the catch signal is to produce a scatter wave. Chang⁴ uses the scatter wave to collect damage data. This wave is the difference between the baseline catch signal (no damage) and damage catch signal. The difference minimizes the reflections from natural boundaries, as seen in Fig. 7.

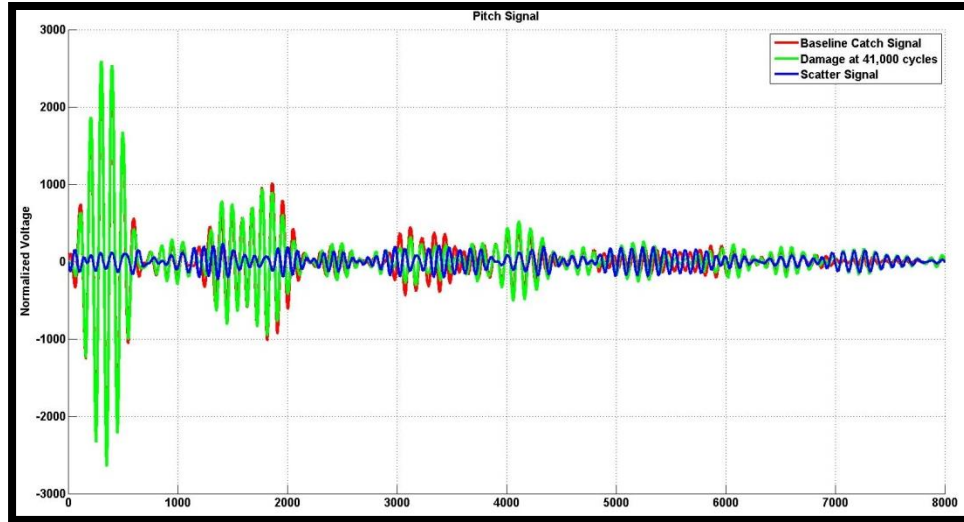


Fig. 7 Scatter signal

The scatter signal carries the change in attenuation as well as phase shift. Chang uses this processes signal to produce a damage index (DI). This index, in turn, through a calibration via linear regression, can potentially indicate damage size.

The scatter signal is only one of many ways to process the damage signal data for DI calculations. The analysis in Section 5 covers a few different DI methodologies based on the scatter signal produced at every pause interval in the procedure.

4. Crack-Length Measurement

A main component of this research project is the capability to measure the true crack length in the dogbone specimen. Others such as Derriso³ have used a traveling microscope to measure the crack length in a specimen. To reduce the amount of manual intervention in the measuring process, a procedure was developed for a Canon T3i camera. The camera is triggered by the MTS software to capture an image of the crack propagation area at every pause for SHM scanning. This synchronization assures that the subsequent DI from the scan corresponds to the measured crack length. The camera is positioned to face one side of the specimen, perpendicular to the surface to the dogbone, as shown in Fig. 8. The lens is focused on the crack propagation area at maximum load (5 kN).



Fig. 8 Camera setup

This area lies to the right of the hole and captures the notch cut created by the jeweler's blade, as shown in Fig. 9. The cut itself is less than 20 mil. Once the camera is focused, its settings are locked. To relate the crack size in the image to the true crack size, a calibration piece is needed to determine a pixel:length ratio. Figure 10 shows the calibration piece used to extract a pixel:inch ratio for crack-length measurement. This is a piece of anodized Al with a black surface finish. The shape was etched onto the Al using a laser engraver. After etching, the piece is then clamped to the specimen with the surface flush with the surface of the specimen. After the focus is adjusted to the crack propagation area, the camera is translated (parallel to the surface of the specimen) so that the visual calibration piece is in full with the prefocused settings. The image is captured and used to generate an inch:pixel ratio.



Fig. 9 Crack propagation area

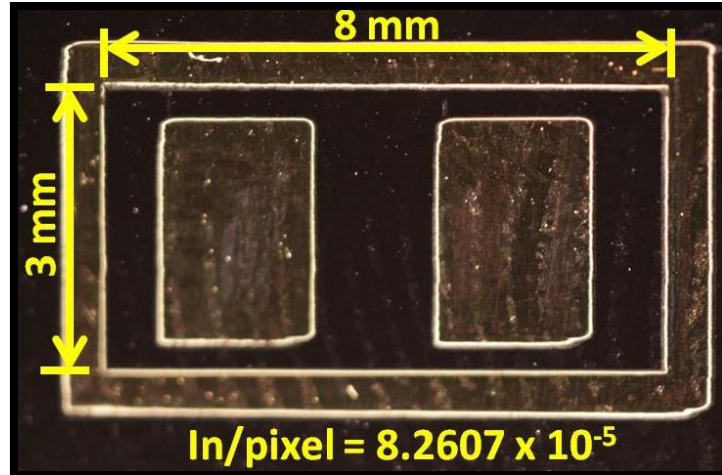


Fig. 10 Visual calibration piece

The translation of the camera is made under the assumption that the plane of the surface of the specimen is parallel to the plane of view of the camera. As can be seen in Figs. 9 and 10, the entire viewing area is not uniformly focused. This could be due to warping of the material or misalignment of the camera plane. Both issues will be addressed in the next report.

In the visual measurement process, a MATLAB script takes in the crack image and inch:pixel ratio and computes the estimated length, as shown in Fig. 11. The location of the crack tip is found by the user by directing the mouse cursor to the crack tip. The process is subject to human error. This issue will be addressed in the next report.

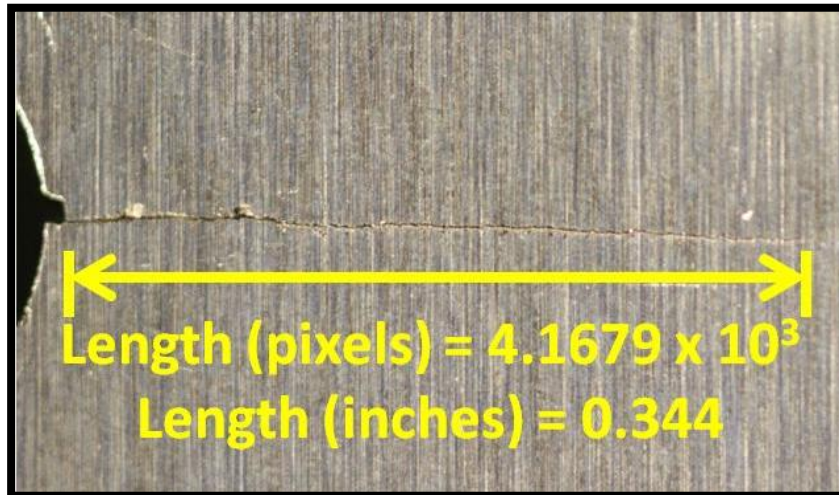


Fig. 11 Example visual measurement

5. Results: DB1

5.1 Crack-Length Images

The A1 dogbone coupon designated DB1 was the first specimen to be tested and scanned using the SMART layer patches. The specimen was run (to failure) for 50,545 cycles at a frequency of 10 Hz and a R value of 0.1 where the maximum load was 5 kN and the minimum load was 500 N. Every 100 cycles, the test stopped and the specimen was held at maximum load for crack image capture and SHM scan.

Processing the visual data using the MATLAB script produced Fig. 12. The first visual detection of a crack occurred at 21,100 cycles. The crack grew outside the camera viewing area after 48,300 cycles. Issues due to inconsistent focus area and low contrast between crack and coupon surface features led to a few data points that were inconsistent with the trend. Future tests will try using white-out to increase the contrast and the visibility of the crack, possibly allowing for an automated crack measurement through MATLAB's image processing toolbox.

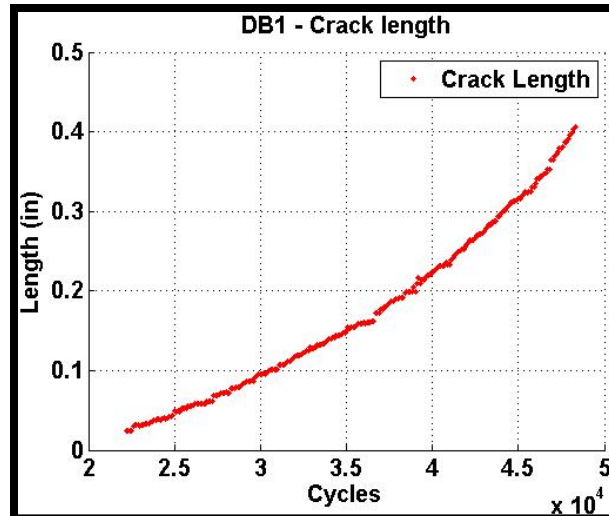


Fig. 12 DB1 measured crack length

5.2 Damage Index Algorithms

Two distinct DI algorithms were explored to examine the sensitivity of the SHM data to visual damage: Chang's signal energy⁴ and Pearson's Correlation Coefficient.⁵ Since SHM Patch outputs data based on each actuator-sensor path (shown in Fig. 4), it is worth investigating which path is more sensitive to actual damage.

Equation 1 provides Chang's energy based DI,⁴ which is defined as a ratio between the energy of the scatter wave in damage signals and the baseline catch wave signal (no damage). The scatter wave, S_{sc} , is the difference between the baseline catch signal and the damage catch signal.⁶ As damage propagates, the difference should increase. This energy ratio is similar to a relative difference calculation. As the difference increases, the ratio tends toward 1.0.

$$Damage\ Index\ (DI) \equiv \left(\frac{\int_{t_i}^{t_f} |S_{sc}(\omega_o, t)|^2}{\int_{t_i}^{t_f} |S_b(\omega_o, t)|^2} \right)^\alpha. \quad (1)$$

In Chang,⁴ alpha was set to 0.5 for its linear response. In Fig. 13 the DI⁴ is shown with respect to cycle count and path as calculated from DB1's SHM scan data.

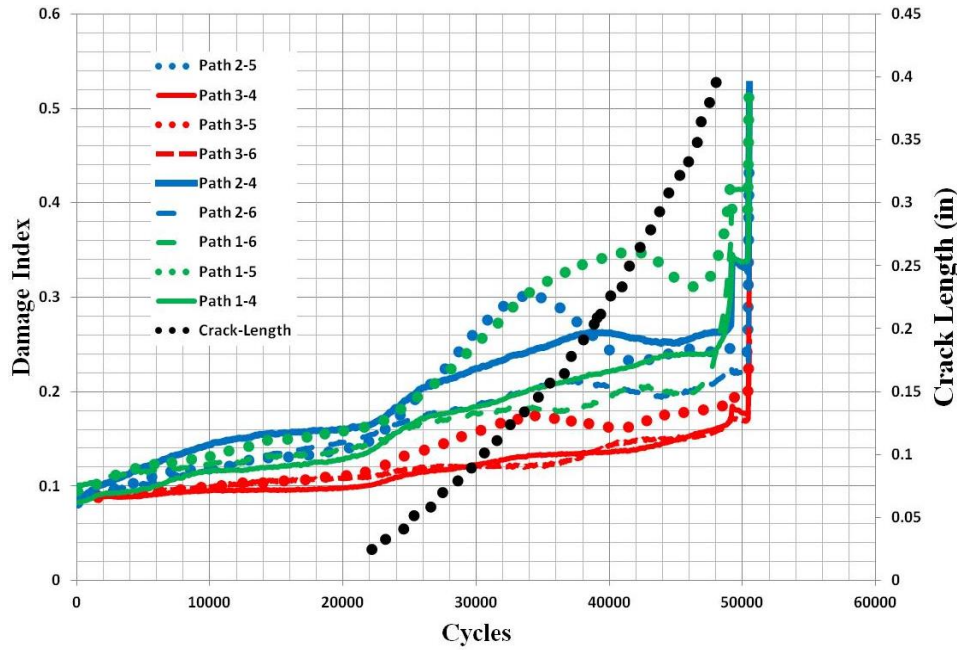


Fig. 13 Scatter wave DI

The paths originating from actuator 1 and 2 are more sensitive to damage than actuator 3. This may be because of the location of the crack. In later studies, this effect could be used as a measure of damage location. The point where the crack becomes visible also coincides with an inflection point in all paths. Path 1-4 showed the most linear trend. Paths 2-5 and 1-5 displayed the most sensitivity due to damage; however, at 40,000 cycles the index drops off significantly. The reason for this is unclear and more studies in the physics of elastic wave propagation should be explored. It is possible that after certain crack length no useful catch signal is transmitted through the coupon.

Vehorn uses Pearson's correlation coefficient,⁵ widely used in the field of statistics, to calculate a DI. The formulation of this index is

$$\text{Damage Index (DI)} = 1 - \rho_{xy}, \quad (2)$$

where ρ_{xy} is the Pearson's coefficient, which is a measure of linear correlation between 2 sets of data. In this case the 2 sets are the damage catch signal and baseline catch signal. If there is no damage, both signals should be identical, producing a correlation of 1.0. As the damage signal changes the linear correlation decreases (hence the subtraction from 1.0 in Eq. 2). The coefficient itself is determined using

$$\rho_{xy} = \frac{E[(x - \mu_x)(y - \mu_y)]}{\sqrt{\text{Var}(x)}\sqrt{\text{Var}(y)}}, \quad (3)$$

where $E[(x - \mu_x)(y - \mu_y)]$ is the averaging operator, $\sqrt{\text{Var}(x)}$ is the standard deviation operator, and μ_x and μ_y are the means of the data sets, respectively.

Figure 14 displays all the damage indices as formulated by Pearson's coefficient with respect to cycles and path. The sensitivity matches to what was found with Chang's energy ratio.⁴ Paths emanating from actuator 4 did not show significant change as actual damage increased.

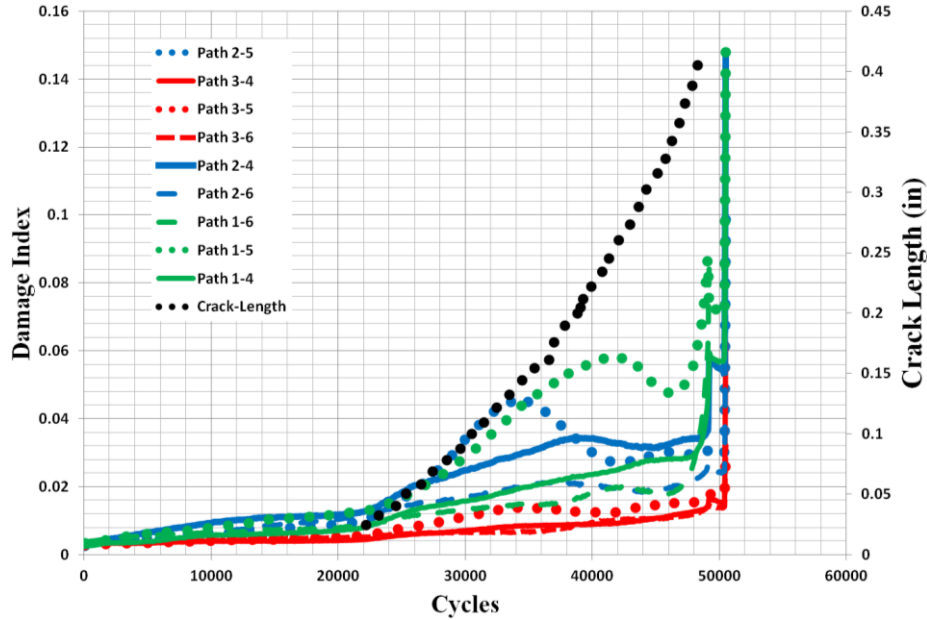


Fig. 14 Pearson's coefficients DI

5.3 Future Work

In future analysis it will be prudent to begin to attempt to use linear regression between the most linearly respondent DI and actual crack length. Another signal aspect, such as frequency, should be explored. It is possible that a different frequency (possibly closer to resonance of the coupon) will induce a more linear DI response. A test including a frequency would help in determining the best frequency to use this particular coupon. It is also possible that as damage evolves in the coupon the resonant frequency changes, necessitating a frequency sweep to produce a significant response.

6 February 2015 Proceedings

The following is a list of action items for February 2015:

- SHM testing of specimen DB2 (see Appendix B).
- Investigation of thermal expansion due to fatigue-induced heating.
- Testing of white-out layer for increased crack image contrast.
- Run multiple scans per crack size.
- Scan at different frequencies (frequency sweep).
- Explore other damage index algorithms.
- Compare and contrast measured crack growth with crack growth models.

7. References

1. Shiao M, Wu Y-T, Ghoshal A, Ayers J, Le D. Probabilistic structural risk assessment for fatigue management using structural health monitoring. Aberdeen Proving Ground (MD): Army Research Laboratory (US); 2012. Internal report.
2. International alloy designations and chemical composition limits for wrought aluminum and wrought aluminum alloys. Arlington (VA): The Aluminum Association; 2001.
3. Derriso M, Little JE II, Vehorn AK, Davies MJ, DeSimio MP. Crack detection using combination of acoustic emission and guided wave signals from bonded piezoelectric transducers. Proceedings of the Eighth International Workshop on Structural Health Monitoring; 2011 Sep 13–15; Stanford, CA. Stanford (CA): Structures and Composites Laboratory (SACL), Department of Aeronautics and Astronautics, Stanford University; c2011. p. 1986–1993.
4. Ihn J-B, Chang F-K. Detection and monitoring of hidden fatigue crack growth using a built-in piezoelectric sensor/actuator network: I. Diagnostics. *Smart Materials and Structures*. 2004;13:609–620.
5. Vehorn AK, DeSimio MP, Olson SE, Brown SK, Leonard MS. Stability of guided wave signals from bonded piezoelectric sensors. In: Kundu T, editor. *Health monitoring of structural and biological systems: Proceedings of SPIE*. 2013 Apr;8695:10 pages. doi: 10.1117/12.2009733.
6. Ihn J-B, Chang F-K. Pitch-catch active sensing methods in structural health monitoring for aircraft structures. *Structural Health Monitoring*. 2008;7(1):5–19.

Appendix A. Experimental Procedure

This appendix appears in its original form, without editorial change.

The following are procedures for fatiguing of 7075-T6 Al (dogbone) with SHM evaluation using SHM Patch

1. Pre-Testing

1.1 *Pumps*

Step 1: In lab atrium move black dot to “IN USE” on the “Process Chilled Water” Board

Step 2: Turn on Process Chilled Water

1.2 *MTS Control*

Step 1: Turn On monitor

Step 2: Open MTS Station Manager Software

Step 3: Open Configuration file: “Setup” and parameter file “setup

Al v6”s

Step 4: Take exclusive control

Step 5: Reset Interlock

Step 6: Turn On Hydraulics (‘HSM’)

Step 7: Start MPT and load method for Fatigue Test & SHM

Step 8: Warm up actuator with $f = 0.1$ Hz and displacement amplitude: 20 mm in displacement mode

1.3 *Specimen Setup*

Step 1: Open bottom grip; move crosshead as needed

Step 2: Place specimen in bottom grip

Step 3: Make sure left side of specimen is aligned with grip guide with not in direct contact (attached to grip)

Step 4: Specimen need not be in contact with the grip bottom.

Close bottom grip

Step 5: Rotate bottom grip so top of specimen is aligned with top grip

Step 6: Adjust crosshead to lower top grip into position

Step 7: Without making contact with bottom of the grip, lower top grip so that top of specimen enters the grasping area of the grip

Step 8: Close top grip

Step 9: Lock Crosshead

Step 10: Go to ‘manual control’ & ‘Force mode’ and zero-out load

Step 11: Record displacement at zero load, Air temperature & Humidity

Step 12: Adhere thermocouple below notch-cut (on specimen) and on the opposite side of the camera view

1.4 *Camera Setup*

Step 1: Take off Lens-cap (camera is pre-positioned)

Step 2: Clear camera memory & reset image numbering

Step 3: Take off Lens caps

Step 4: Attach trigger cable to camera

Step 5: Set camera to the following settings: M-mode, ISO_____,
F-stop_____

Step 6: Turn on light source(s)

Step 7: Adjust camera view & zoom to the space between the edge of the hole and one side (this is the ‘notched’ side of the hole where the crack will propagate)

Step 8: Adjust light to appropriate saturation levels

1.5 SHM Patch Sensor & Thermocouple Sensor Setup

Step 1: Attach cable labeled ‘CH.1’ to Top SHM Patch lead (this is the actuator sensor)

Step 2: Attach cable labeled ‘CH.2’ to Bottom SHM Patch lead (sensing sensor)

Step 3: Make sure cables are not in the camera view

Step 4: Let Temperature reading stabilize for 5 min

2. Fatigue Test & SHM Procedure

2.1 Baseline Picture

Step 1: Apply the High Load to the specimen (crack documentation occurs at high load)

Step 2: Check for camera support for vibrations & adjust focus.

Step 3: Check Memory. Pictures should be labeled: IMG_00##

Step 4: Take Baseline Picture with image calibration piece

2.2 Pre-fatigue checks & Baseline SHM Scan

Step 1: Check SHM Patch sensor impedance level & adjust appropriately

Step 2: Run SHM Patch ‘Integrity Check’

Step 3: Take several baseline scans in SHM Patch software @ high load (without damage)

Step 4: Check signal quality and adjust gain as needed

Step 4: Reset Cycle count in ‘cycle.mat’ to 0 cycles

Step 5: set scanning parameters in ‘SHM_Scan.mat’ to desired values (i.e. Specimen #)

Step 6: Change data folder name, “E#”, to appropriate Specimen #

Step 7: Write/record start time & displacement @ zero load

*2.3 Automated Crack Growth Procedure***

Step 1: Begin thermocouple data acquisition

Step 2: Start MTS method and run for 100 cycles

Step 3: Stop cyclical load and ramp up to max load (5kN – high, 500N low, f = 10Hz)

Step 4: Take Picture*

Step 5: Take SHM scan & Record Data

Step 6: Repeat steps 2-5 until failure

2.4 *Post Failure*

Step 1: Go to manual control (+displacement control mode)

Step 2: Remove Specimen

Step 3: Turn off Hydraulics

Step 4: Turn off chilled water pump (& move dot to “not in use”)

Step 5: Collect Load/Displacement/Cycle Count/Temperature/
SHM Data

*Record, separately, the running cycle time, image, and any events (Crack Initiation, Failure, etc...) for later reference and image processing

** Steps 2-5 are programmed as an automated procedure on the MTS Station Manager Software

Testing notes

- At every pause scan dogbone _____ times
- Before test at least _____ baseline SHM scans will be taken
- Hole in specimen will have a notch cut of length < 20 mils made by jewelers saw blade

Appendix B. Setup for Crack Image Capture for Dogbone 2



Fig. B.1 Camera translation stage

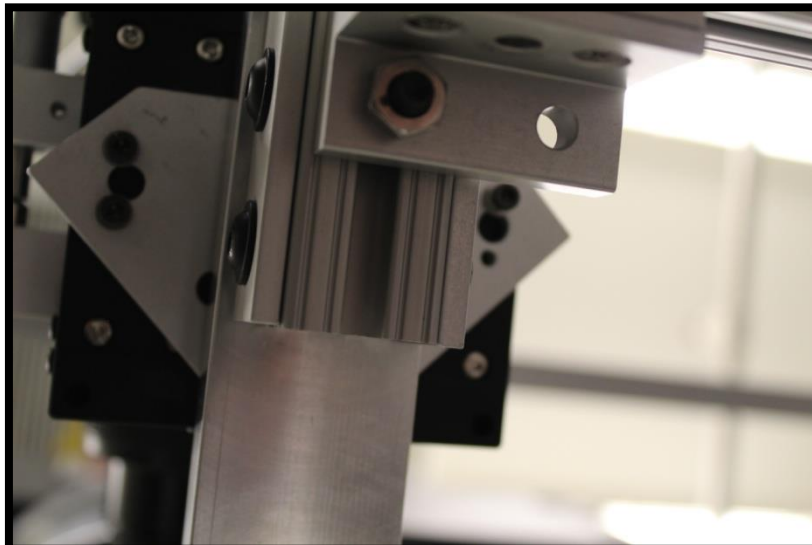


Fig. B.2 Bottom view of camera translation stage



Fig. B.3 White-out application

INTENTIONALLY LEFT BLANK.

List of Symbols, Abbreviations, and Acronyms

Al	aluminum
DB	dogbone
DI	damage index
CBM	condition-based maintenance
NDI	nondestructive inspection
POD	probability of detection
PSRA	probabilistic structural risk assessment
PZT	piezoelectric transducer
SHM	structural health monitoring

1 DEFENSE TECHNICAL
(PDF) INFORMATION CTR
DTIC OCA

2 DIRECTOR
(PDF) US ARMY RESEARCH LAB
RDRL CIO LL
IMAL HRA MAIL & RECORDS
MGMT

1 GOVT PRINTG OFC
(PDF) A MALHOTRA

3 USARL
(PDF) RDRL VTM
R HAYNES
E IGLESIAS
RDRL VTP
C SHIAO